Analysis of the application value of SUV in quantitative SPECT/CT for diagnosing benign and malignant bone lesions

Jun Guo[1#] MD,
Chi Chen[1#] MD,
Linlin Xiong[2] MD,
Liang Xiao[1] MD,
Yuxi Wei[1] MD,
Chen Sun[2] MD

1. Department of Traumatic orthopedics, Renmin Hospital, Hubei University of Medicine, Shiyan, Hubei 442000, China
2. Department of Obstetrics and Gynecology, Shiyan Matenal and Child Health Hospital, Shiyan, Hubei, China
3. Wuhan Jinyintan Hospital, Trauma Center Affiliated to Tongji Medical College of Huazhong University of Science and Technology; Hubei Clinical Research Center for Infectious Diseases; Wuhan Research Center for Communicable Disease Diagnosis and Treatment, Chinese Academy of Medical Sciences; Joint Laboratory of Infectious Diseases and Health, Wuhan Institute of Virology and Wuhan Jinyintan Hospital, Chinese Academy of Sciences, Wuhan, 430023, China

Keywords: Quantitative SPECT/CT - SUV - Differential diagnosis - Benign and malignant bone lesions - Application value

Corresponding author:
Chen Sun MD,
Wuhan Jinyintan Hospital, Trauma Center Affiliated to Tongji Medical College of Huazhong University of Science and Technology; Hubei Clinical Research Center for Infectious Diseases; Wuhan Research Center for Communicable Disease Diagnosis and Treatment, Chinese Academy of Medical Sciences; Joint Laboratory of Infectious Diseases and Health, Wuhan Institute of Virology and Wuhan Jinyintan Hospital, Chinese Academy of Sciences, Wuhan, 430023, China
36865718@qq.com

Received:
6 September 2024
Accepted revised:
18 November 2024

Abstract

Objective: To analyze the application value of standardized uptake value (SUV) in quantitative single-photon emission computed tomography/computed tomography (SPECT/CT) based on the maximum expectation reconstruction algorithm for diagnosing benign and malignant bone lesions. **Subjects and Methods:** A retrospective analysis was conducted on the clinical data of 83 patients suspected of bone metastasis who underwent quantitative SPECT/CT bone scans in our hospital from September 2023 to July 2024. A total of 91 high-metabolic bone lesions were outlined for SUV measurement, while the spinal SUV of patients with normal bone metabolism were outlined as the control group (46 vertebral bodies). The maximum SUV (SUVmax), mean SUV (SUVmean), and minimum SUV (SUVmin) of benign lesions (benign group), malignant lesions (malignant group), and the control group were measured and compared. Receiver operating characteristic (ROC) curves were plotted to analyze the diagnostic value of SUV in differentiating benign and malignant bone lesions using quantitative SPECT/CT. **Results:** Based on the final diagnosis determined by pathology and/or imaging follow-up for 6-12 months or more, 50 malignant bone lesions and 41 benign bone lesions were identified. The levels of SUVmax, SUVmean, and SUVmin in the malignant and benign groups were higher than those in the control group, with the malignant group showing higher levels than the benign group ($P<0.05$). Receiver operating characteristic curve analysis showed that the areas under the curves for SUVmax, SUVmean, and SUVmin were 0.867, 0.909, and 0.896, respectively. The optimal cut-off value for SUVmax was 26.58g/mL, with a specificity of 100% and a sensitivity of 65.27%; for SUVmean, the optimal cut-off value was 12.75g/mL, with a sensitivity of 78.36% and a specificity of 93.54%; for SUVmin, the optimal cut-off value was 9.13g/mL, with a sensitivity and specificity of 81.42% and 89.87%, respectively. The diagnostic detection rate of quantitative SPECT/CT fusion imaging combined with SUVmean analysis (91.21%) was higher than that of conventional SPECT/CT fusion imaging qualitative analysis (74.73%) ($P<0.05$). **Conclusion:** Standardized uptake value in quantitative SPECT/CT to some extent supplements the qualitative analysis of tumor bone metastasis and benign bone lesions, offering a higher accuracy in diagnosing tumor bone metastasis and differentiating between benign and malignant lesions compared to conventional SPECT/CT bone fusion imaging.

Hell J Nucl Med 2024; 27(3): 198-205 *Epub ahead of print: 14 December 2024* *Published online: 30 December 2024*

Introduction

In clinical practice, bones are one of the common sites for malignant tumor metastasis. Once bone metastasis occurs, patients face a significantly increased risk of bone-related events, such as pathological fractures, spinal cord compression syndrome, and hypercalcemia. These events not only severely affect patients' quality of life but may also shorten their survival time [1, 2]. Therefore, early detection and accurate diagnosis of bone metastasis are crucial for timely treatment planning, delaying disease progression, and improving patients' quality of life. Radionuclide bone imaging, widely used in current clinical practice, provides a sensitive and cost-effective method for early diagnosis of bone metastasis by assessing the functional metabolic status and structural changes of the entire skeletal system [3]. However, traditional radionuclide bone imaging primarily relies on qualitative analysis. Although it offers high sensitivity and low cost, its diagnostic accuracy remains limited when faced with atypical imaging presentations of bone metastases [4]. With the continuous advancement of imaging technology, single photon emission computed tomography/computed tomography (SPECT/CT) has emerged, combining the functional imaging of SPECT with the anatomical imaging of CT, thereby gradually enhancing the diagnostic performance of tumor bone metastasis [5]. However, diagnosing certain atypical concentrated lesions remains challenging with SPECT/CT, making it crucial to improve the diagnostic capabilities of radionuclide imaging.

The emergence of quantitative nuclear medicine technology offers a new solution to this challenge. By introducing standardized uptake value (SUV) as a quantitative indicator, quantitative SPECT/CT not only overcomes the subjectivity of traditional visual interpretation but also provides more objective and precise quantitative analysis, significantly enhancing the accuracy of image diagnosis [6]. As a quantitative evaluation index, SUV can quantify the bone mineral metabolism of lesions, aiding in the better identification and diagnosis of suspected bone metastases and improving the precision of lesion differentiation [7]. In recent years, several studies [8, 9] have confirmed the feasibility and clinical application potential of SUV in quantitative SPECT/CT. Based on this background, this study aims to systematically evaluate the diagnostic value of SUV in quantitative SPECT/CT fusion imaging, particularly exploring its application potential in differentiating benign from malignant bone lesions. Compared with conventional SPECT/CT, this study is the first to analyze the advantages of quantitative SPECT/CT combined with SUV in clinical diagnosis from multiple perspectives, focusing on its ability to differentiate bone metastases with atypical imaging presentations or without significant changes in bone density. This study not only contributes to improving the diagnostic accuracy of bone metastases but also provides new diagnostic strategies for clinical practice, offering strong support for treatment decision-making in patients with malignant tumors.

Subjects and Methods

Study subjects and inclusion criteria

A retrospective analysis was conducted on the clinical data of 83 patients with suspected bone metastasis who underwent quantitative SPECT/CT bone scans in our hospital between September 2023 and July 2024. Inclusion criteria: 1) Underwent whole-body bone imaging and tomographic imaging using SPECT/CT; 2) Imaging data from tumor or non-tumor patients showed hypermetabolic lesions; 3) Complete and authentic clinical data available for analysis. Exclusion criteria: 1) Currently undergoing targeted or endocrine therapy; 2) Recent history of radiotherapy or chemotherapy within the last month; 3) Unable to remain in a supine position for an extended period; 4) Women who are breastfeeding and/or pregnant; 5) Unable to fully participate in the study and/or with incomplete clinical data. Among the 83 patients with suspected bone metastasis, there were 40 males and 43 females, aged 14-80 years, with an average age of (57.24±10.38) years. The diagnoses included 31 cases of lung cancer, 14 cases of nasopharyngeal cancer, 10 cases of breast cancer, 5 cases of prostate cancer, 3 cases each of thyroid cancer and gastric cancer, 2 cases each of sigmoid colon cancer, rectal cancer, laryngeal cancer, and esophageal cancer, 1 case each of kidney cancer, duodenal cancer, ovarian cancer, large cell medulloblastoma, and cervical cancer, and 4 cases of non-tumor. This study was approved by the Medical Ethics Committee.

Imaging method

Patients first received an intravenous injection of technetium-99m-methylene diphosphonate (^{99m}Tc-MDP) at a dose controlled between 555-925MBq (approximately 15-25mCi). To ensure the accuracy of the injected dose, the full needle activity in the syringe was recorded before injection, and the residual activity in the syringe was measured after injection. The time of injection was also recorded, which helped accurately calculate the actual radioactive dose administered to the patient. Imaging was performed 3-4 hours post-injection to ensure sufficient distribution and accumulation of the drug in the bone tissue. The imaging was conducted using a dual-head γ camera equipped with a parallel-hole low-energy high-resolution collimator. The scanning parameters were set as follows: matrix 128×128, magnification 1.0. Each detector rotated 180°, with a 10° interval per frame, and an exposure time of 7 seconds per frame, totaling 36 frames. The counts per frame were controlled between 1500-2000 Kcounts to ensure high-quality image data. Subsequently, patients underwent CT scans using a 16-slice spiral CT scanner. The CT parameters were set to a scan width of 40 cm, matrix size of 512×512, voltage of 120kV, current of 180mA, and slice thickness of 3.75mm. These parameters were chosen to balance spatial resolution with radiation dose, ensuring sufficient anatomical detail for accurate lesion localization and analysis. All imaging data were transferred to the Discovery NM/CT 670 (GE) system's post-processing workstation for further processing. During processing, images were reconstructed using the three-dimensional ordered subset expectation maximization (3D-OSEM) method, with two iterations set for the reconstruction process.

Image analysis and diagnostic criteria

In this study, image data analysis was jointly conducted by two senior nuclear medicine physicians from our department, both holding associate senior titles or above. To ensure the accuracy and standardization of image interpretation, the physicians independently assessed all images and performed detailed analysis for each case. In cases where there were discrepancies in their diagnostic opinions, they would discuss and reach a consensus on the final diagnosis. The image analysis process was divided into two stages. First, the physicians conducted a preliminary evaluation of the whole-body bone scan images to identify potential bone lesions. Next, they performed a more in-depth analysis of the SPECT/CT fusion images to interpret the hyper-concentrated lesions in greater detail. Based on imaging findings, the lesions were preliminarily classified into the following categories: benign bone lesions (e.g., fractures, degenerative changes, inflammation, infections by specific pathogens, etc.), metastatic bone tumors, or lesions of uncertain diagnosis (requiring follow-up for confirmation). All preliminary diagnostic results required a 6-12 month follow-up to ensure diagnostic accuracy. During the follow-up period, the research team regularly reviewed the imaging data of the enrolled patients, including whole-body bone scans, X-rays, SPECT/CT, CT, and magnetic resonance imaging (MRI), among other imaging modalities. Additionally, pathological biopsy results were also considered to further verify the final diagnosis corresponding to the lesions identified by radio-

nuclide imaging. The diagnostic criteria for bone metastases included the following key factors: First, the presence of hyper-concentrated lesions in areas such as the spine, ribs, sternum, scapula, clavicle, or long bones, with asymmetry and irregular shapes. In the SPECT/CT fusion images, these lesions presented as osteolytic or osteoblastic bone destruction, strongly suggesting malignancy [10]. In contrast, the diagnosis of benign lesions was based on different imaging characteristics. Benign lesions usually appeared in surgical sites or areas with a clear history of trauma, or were found in known benign bone conditions (e.g., bone hyperplasia, sclerosis, vertebral compression fractures, etc.). Additionally, certain physiological uptake areas (e.g., sternoclavicular joints, costal cartilage, etc.) were also considered benign lesions. In the SPECT/CT fusion images, benign lesions typically did not exhibit osteolytic or osteoblastic bone destruction, and there were no soft tissue mass shadows surrounding them [11].

To enhance clarity, Figures 1-2 provides a flowchart of the patient selection and imaging process, illustrating the criteria for inclusion and exclusion as well as the imaging and diagnostic procedures followed in this study.

Statistical analysis

GraphPad Prism 8 software was used for graphing, and SPSS 22.0 software was used for data processing. Categorical data were expressed as [n (%)], and the chi-square test was used for analysis. Measurement data following a normal distribution were expressed as $\bar{x} \pm s$, and independent sample t-tests were used for comparison between groups, while F-tests were used for comparison among three groups. Receiver operating characteristic (ROC) curves were drawn to analyze the diagnostic value of SUV in quantitative SPECT/CT for distinguishing between benign and malignant bone lesions. A P-value of less than 0.05 was considered statistically significant.

Results

Comparison of SUV levels among the three groups

Through pathological examination and/or imaging follow-up of 6 to 12 months or longer, a total of 91 bone hyperme-

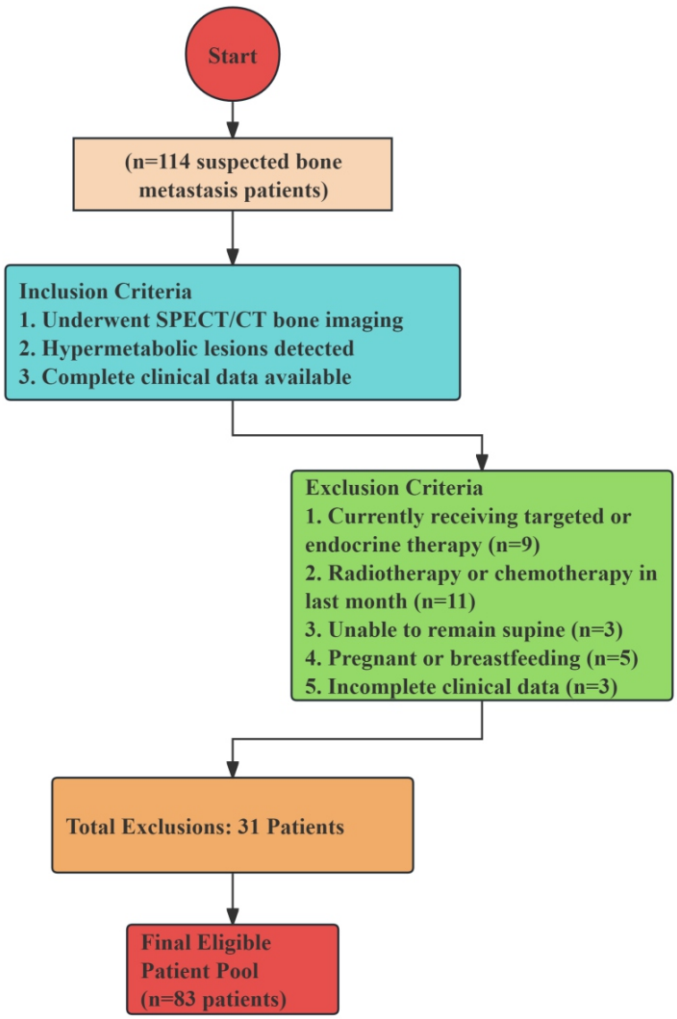

Figure 1. Patient selection flowchart.

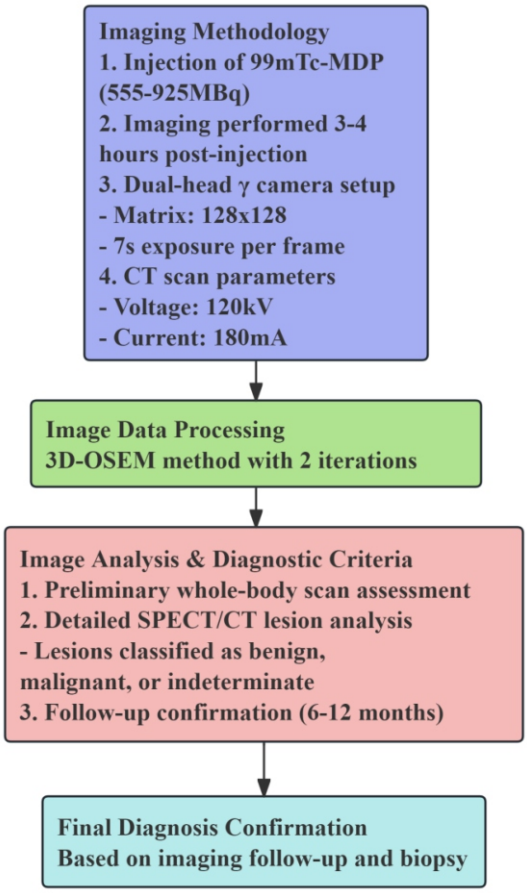

Figure 2. Imaging process flowchart.

tabolic lesions were diagnosed, of which 50 were confirmed as malignant lesions, all being metastatic bone tumors. Among the 41 benign lesions, further classification revealed that 15 lesions were caused by fractures, and the remaining 26 were non-fracture lesions. These non-fracture lesions included 17 cases of osteoarthritis and degenerative changes, 2 cases of femoral head necrosis, and 7 other benign lesions.

At the initial diagnosis stage, SPECT/CT scans were performed on all untreated patients. To quantify the level of radioactive uptake in abnormal bone metabolism areas, the research team used specialized quantification software to outline the range of each bone hypermetabolic area and, based on follow-up results, classified these lesions into a malignant group (n=50) and a benign group (n=41). As a control, areas of normal metabolic spine regions (n=46) were selected, and the areas with the highest concentration of radioactivity were outlined, taking the area of maximum radionuclide concentration as the center and obtaining the corresponding SUV along the bone's boundary. Subsequently, the maximum SUV (SUVmax), mean SUV (SUVmean), and minimum SUV (SUVmin) values of lesions in the three groups were measured. The results showed that the differences in these SUV values among the malignant group, benign group, and control group were statistically significant ($P<0.05$). Specifically, the SUV values showed a progressively decreasing trend across the three groups, with the highest SUV values in the malignant lesion group, followed by the benign lesion group, and the lowest in the control group, as shown in Table 1.

Diagnostic value of SUV levels for malignancy in bone lesions

Using SUVmax, SUVmean, and SUVmin as test variables, and the benign/malignant nature of the bone lesions (No=0, Yes=1) as the status variable, ROC curves were plotted. The results showed that the area under the curve (AUC) for SUVmax, SUVmean, and SUVmin were 0.867, 0.909, and 0.896, respectively, as detailed in Table 2 and Figure 3.

Diagnostic value between conventional SPECT/CT fusion images and quantitative SPECT/CT fusion images and SUVmean

The diagnosis of the 91 bone hypermetabolic lesions included in this study was confirmed through a 6 to 12-month follow-up, which included whole-body bone scans, CT, MRI, SPECT/CT, and pathological verification. At the initial diagnosis stage, among these 91 lesions, 41 were diagnosed as metastatic bone tumors, 27 as benign lesions, and the remaining 23 lesions could not be definitively diagnosed due to atypical imaging features. For these 23 lesions that could not be definitively diagnosed, the research team conducted close follow-up, and through subsequent imaging examina-

Table 1. *Comparison of SUV levels among the three groups ($\bar{x} \pm s$)*

Group (n)	SUVmax	SUVmean	SUVmin
Malignant group (n=50)	30.12±8.79*#	16.62±5.09*#	11.62±3.42*#
Benign group (n=41)	13.47±3.62*	8.26±1.35*	5.79±1.18*
Control group (n=46)	7.45±1.98	3.73±0.69	1.04±0.47
F	198.245	202.289	283.039
P	<0.01	<0.01	<0.01

*Note: Compared with the control group, *P<0.05; compared with the benign group, #P<0.05.*

Table 2. *Diagnostic value of SUV levels for malignancy in bone lesions.*

Index	Cut-off value	AUC	95% CI	P	Sensitivity (%)	Specificity (%)
SUVmax	26.58g/mL	0.867	0.801~0.945	＜0.05	100.00	65.27
SUVmean	12.75g/mL	0.909	0.853~0.976	＜0.05	78.36	93.54
SUVmin	9.13g/mL	0.896	0.842~0.959	＜0.05	81.42	89.87

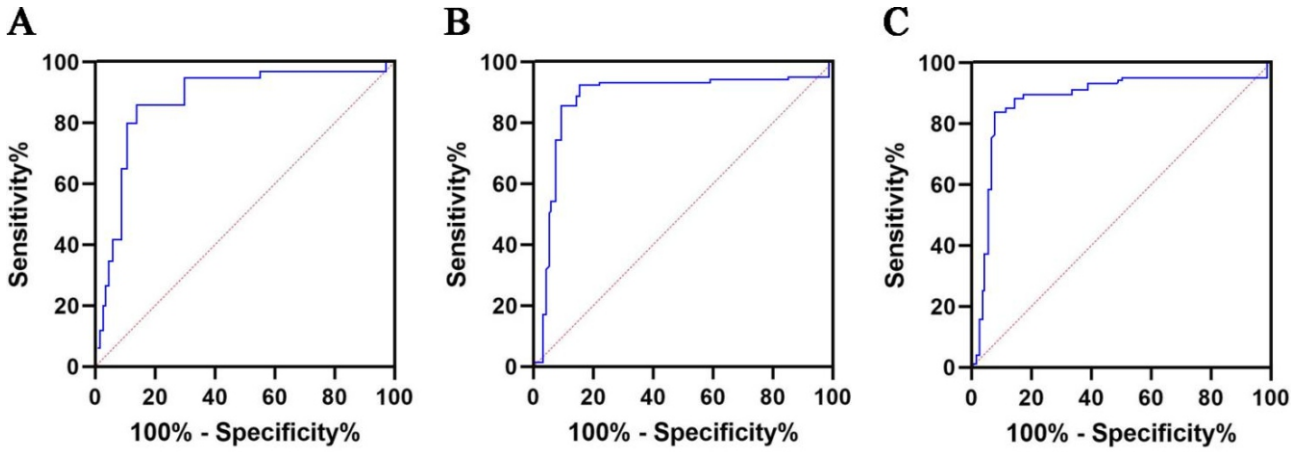

Figure 3. ROC curve analysis of SUV levels for diagnosing bone lesion malignancy. A: SUVmax; B: SUVmean; C: SUVmin.

tions and pathological analysis, 9 were eventually diagnosed as metastatic bone tumors, and 14 as benign lesions. A comprehensive analysis of these follow-up results confirmed that out of the 91 bone hypermetabolic lesions, 50 were metastatic bone tumors and 41 were benign lesions, with the research results detailed in Table 3.

An in-depth analysis was conducted on the 91 bone hypermetabolic lesions included in this study, dividing them into two groups for comparative research. The first group's analysis was performed by an experienced nuclear medicine physician at a workstation, where the physician independently read the images and made preliminary judgments on the lesions based on their experience, categorizing them into four types: benign, possibly benign, possibly malignant, and malignant. According to the preliminary judgment results, these lesions were classified into two diagnostic results: Diagnostic Result 1: lesions that could be definitively diagnosed, including metastatic bone tumors and benign lesions (e.g., degenerative changes, inflammation, fractures); Diagnostic result 2: lesions that could not be definitively diagnosed, which included possibly benign lesions, bone metastasis could not be ruled out, possibly bone metastasis, and lesions of uncertain nature. On this basis, the conventional SPECT/CT fusion image analysis results showed that 69 lesions could be definitively diagnosed, while 22 lesions could not be definitively diagnosed.

The second group's analysis was based on qualitative analysis of conventional SPECT/CT fusion images, combined with the best indicator of quantitative analysis, i.e., SUVmean≥ 12.75g/mL as the standard for determining malignant lesions. The 91 lesions were reclassified, and the final follow-up results

were used as the standard for verification. The diagnostic results of this group were also divided into two categories: Diagnostic Result 1: lesions that could be definitively diagnosed (including metastatic bone tumors and benign lesions such as degenerative changes, inflammation, fractures); Diagnostic result 2: lesions that could not be definitively diagnosed. By comparing the diagnostic efficacy of qualitative analysis of conventional SPECT/CT fusion images and quantitative SPECT/CT fusion images+SUVmean analysis, the results showed that the diagnostic detection rate of quantitative SPECT/CT fusion images+SUVmean analysis was 91.21%, significantly higher than that of conventional SPECT/CT fusion image qualitative analysis (74.73%) (P<0.05). Detailed results are shown in Table 4.

Discussion

With the continuous advancement of science and technology, particularly in the field of medicine, nuclear medicine examination techniques have also seen significant development. The SPECT/CT equipment, by integrating anatomical imaging with CT and functional imaging techniques, has made the diagnosis of bone metastases more accurate and reliable [12]. However, in clinical practice, doctors still need to invest considerable time in identifying bone metastatic lesions on SPECT/CT images. The accuracy and sensitivity of this process often depend on the physician's experience, which carries a certain degree of subjectivity and lacks systematic quantitative analysis methods [13]. The quantitative analysis of SUV in SPECT/CT provides an effective solution to this diagnostic challenge. By quantifying the high metabolic bone metastatic lesions, the SUV value can objectively reflect the metabolic characteristics of bone metastatic lesions [14]. More importantly, different nuclear medicine physicians have high reproducibility in measuring SUV values, significantly reducing diagnostic inconsistencies caused by individual differences [15]. The results of this study show that the SUV value in quantitative SPECT/CT has significant clinical advantages in distinguishing tumor bone metastases from benign bone lesions (such as fractures, arthritis or degenerative changes in the spine and pelvis, and arthritic changes in the limbs), thus improving the specificity of radionuclide bone scans. The research data indicate that the differences in SUV values between the malignant bone metastasis group, the benign lesion group, and the control group are statistically significant (P<0.05), with the SUV values showing a gradual decreasing trend among these three groups. This result is consistent with the conclusions of previous literature [16]: bone metastatic lesions in malignant tumors often have higher SUV values. Additionally, this study further found that SUVmax, SUVmean, and SUVmin in the malignant group were significantly higher than those in the benign group, indicating that SUV quantitative analysis has important clinical value in the differential diagnosis of benign and malignant lesions. The ROC curve analysis results show that the area under the curve (AUC) for SUVmax, SUVmean, and SUVmin were 0.867, 0.909, and 0.896, respectively, all close to 90%, indicating that these SUV indicators have high diagnostic efficacy and good reproducibility in distinguishing metastatic bone tumors from benign lesions, making them a relatively reliable diagnostic method. Therefore, it is recommended to use SUV measurements to assist in diagnosing bone metastases when performing qualitative analysis of SPECT/CT concentrated lesions, rather than relying solely on the physician's clinical experience or visual judgment. Regarding the recent critical SUV value, relevant studies [17, 18] indicate that the maximum cutoff value for diagnosing metastatic bone tumors is SUVmax ≥20 and SUVmax ≥19.5, which is generally consistent with the results of this study. Nonetheless, there are still some deviations in the optimal diagnostic thresholds between different studies, which may be related to factors such as lesion size, pathological type, and differences in the selection of quantitative instruments and methods. Therefore, in actual clinical practice, the diagnostic threshold of SUV values should be adjusted according to specific conditions to

Table 4. *Comparison of diagnostic value between conventional SPECT/CT fusion image qualitative analysis and quantitative SPECT/CT fusion image and SUVmean analysis.*

Diagnostic method	Definitive diagnosis		Indeterminate diagnosis	Overall diagnostic concordance
	Bone metastasis	Benign lesions		
Conventional SPECT/CT fusion image Qualitative analysis	41 (45.05)	27 (29.68)	23 (25.27)	68 (74.73)
Quantitative SPECT/CT fusion image + SUVmean analysis	46 (50.55)	37 (40.66)	8 (8.79)	83 (91.21)
x^2	-	-	-	8.748
P	-	-	-	0.003

ensure its applicability in different patient populations. Overall, the application of SUV quantitative analysis provides strong support for improving the diagnostic accuracy of metastatic bone tumors and is of great significance in optimizing the diagnostic process of nuclear medicine imaging.

Quantitative SPECT/CT fusion imaging has demonstrated significant technological advances in the field of nuclear medicine imaging, particularly in improving spatial resolution [19]. By reducing the radioactive interference caused by surrounding tissue structures, quantitative SPECT/CT can more accurately display the presence of deep and small lesions [20]. This technology not only enhances lesion visibility but also evaluates the benign and malignant nature of lesions through digital quantitative indicators (such as SUV values), providing more precise evidence for clinical diagnosis, in line with the development trend of modern precision medicine [21]. In recent years, studies [22-24] have found that the three-dimensional ordered-subset expectation maximization (3D-OSEM) reconstruction algorithm based on CT attenuation correction and scatter correction is superior in quantitative accuracy to traditional two-dimensional ordered-subset expectation maximization (2D-OSEM) and filtered back-projection (FBP) reconstruction methods. Choosing the appropriate OSEM reconstruction parameters can significantly improve the quantitative accuracy of SPECT/CT. This study adopted 3D-OSEM reconstructed images and performed two iterations, showing an improvement in quantitative accuracy. However, how to further optimize the OSEM reconstruction parameters to obtain more accurate SUV values remains an important direction for future research.

This study confirmed the high effectiveness of quantitative SUV in SPECT/CT in distinguishing between benign and malignant bone lesions. To further explore the feasibility of quantitative SPECT/CT fusion imaging combined with SUVmean in quantitative analysis, this study compared the diagnostic effects of conventional SPECT/CT fusion imaging with quantitative SPECT/CT fusion imaging + SUVmean. The results showed that the detection rate of metastatic bone tumors with conventional SPECT/CT qualitative analysis was 45.05%, the detection rate of benign lesions was 29.68%, and the proportion of cases that could not be definitively diagnosed reached 25.27%. In contrast, the diagnostic detection rate of quantitative SPECT/CT fusion imaging combined with SUVmean analysis was significantly improved, with the detection rate of metastatic bone tumors reaching 50.55%, the detection rate of benign lesions being 40.66%, and the proportion of cases that could not be definitively diagnosed decreasing to 8.79%. Overall, the total diagnostic detection rate of quantitative SPECT/CT fusion imaging + SUVmean analysis was 91.21%, significantly higher than the 74.73% of conventional SPECT/CT fusion imaging qualitative analysis ($P< 0.05$), indicating that quantitative analysis combined with SUVmean has higher gain value in clinical diagnosis. These results not only validate the potential of quantitative SPECT/CT in clinical applications but also provide important reference data for its future optimization and application. With further research and optimization of quantitative analysis techniques, SPECT/CT is expected to play a greater role in the diagnosis of bone tumors and other related lesions, advancing nuclear medicine imaging towards greater precision.

In conclusion, this study compared the diagnostic results of conventional SPECT/CT qualitative analysis and quantitative SPECT/CT fusion imaging combined with SUVmean analysis. The study showed that the latter was significantly superior in diagnostic accuracy and reliability, suggesting that the introduction of SUVmean not only improved the detection rate of metastatic bone tumors but also significantly reduced the proportion of cases that could not be definitively diagnosed. This indicates that quantitative SPECT/CT combined with SUV analysis can provide more accurate and reliable diagnostic evidence for clinical practice, helping to improve the accuracy and specificity of bone lesion diagnosis. In addition, the study also verified the effectiveness of the three-dimensional ordered-subset expectation maximization (3D-OSEM) reconstruction algorithm based on CT attenuation correction and scatter correction, further consolidating the application foundation of quantitative SPECT/CT in nuclear medicine. Overall, The results of this study hold significant promise for clinical practice. By enabling objective, quantitative assessment of bone lesions, SUV values can reduce dependency on subjective evaluations, there by standardizing diagnostic approaches and reducing interobserver variability. This method can facilitate earlier and more accurate treatment interventions for metastatic bone tumors, potentially improving patient outcomes. As nuclear medicine continues to evolve, quantitative SPECT/CT with SUV measurements may serve as an important diagnostic tool, aligning with the goals of precision medicine to offer individualized patient care. However, it should be noted that this study still has some limitations: 1) Limited sample size: This study included only 91 high-metabolic lesions, with a relatively small sample size, which may affect the generalizability of the results; 2) Single-center study: The data in this study were sourced from a single medical center, which may be subject to regional and departmental operational habits, limiting the generalizability of the results; 3) Selection of quantitative analysis parameters: The 3D-OSEM reconstruction parameters used in this study underwent two iterations, but more extensive parameter optimization research has not yet been conducted, and different parameter settings may affect the accuracy of SUV values; 4) Lack of long-term follow-up data: Although this study conducted 6-12 months of follow-up, it did not cover longer-term follow-up data. Long-term follow-up is helpful in further confirming the long-term reliability and stability of quantitative SPECT/CT in diagnosing different types of lesions; 5) Limited discussion of SUV cut-off values: The discussion of SUV cut-off values in this study was limited, and different studies may have varying cut-off values. Overall, this study provides strong evidence for the application of SUV in quantitative SPECT/CT in the diagnosis of bone lesions, but further optimization and validation are still needed to ensure its widespread application and reliability in clinical practice.

Bibliography

1. Clézardin P, Coleman R, Puppo M et al. Bone metastasis: mechanisms, therapies, and biomarkers. *Physiol Rev* 2021; 101(3): 797-855.

2. Satcher RL, Zhang XH. Evolving cancer-niche interactions and therapeutic targets during bone metastasis. *Nat Rev Cancer* 2022; 22(2): 85-101.
3. Salmon P, Alavi F, Ghasem-Zadeh A. Editorial: Quantitative bone imaging methods. *Front Endocrinol (Lausanne)* 2024; 15: 1411512.
4. Vaz S, Usmani S, Gnanasegaran G et al. Molecular imaging of bone metastases using bone targeted tracers. *Q J Nucl Med Mol Imaging* 2019; 63(2): 112-28.
5. Ritt P, Kuwert T. Quantitative SPECT/CT-Technique and Clinical Applications. *Recent Results Cancer Res* 2020; 216: 565-90.
6. Halim F, Yahya H, Jaafar KN et al. Accuracy Assessment of SUV Measurements in SPECT/CT: A Phantom Study. *J Nucl Med Technol* 2021; 49(3): 250-5.
7. Yoshimura M, Kugai N, Aida T et al. Comparison of bone SUV obtained from different SPECT/CT systems. *Hell J Nucl Med* 2023; 26(3): 181-6.
8. Yamazaki K, Nishii R, Maeda T et al. Assessment of SPECT-CT fusion images and semi-quantitative evaluation using SUV in ^{123}I-IMP SPECT in patients with choroidal melanoma. *Ann Nucl Med* 2020; 34(11): 864-72.
9. Koukouraki S, Kapsoritakis N, Bourogianni O et al. SPECT/CT SUV-based metrics: A promising diagnostic tool in classifying patients with suspected transthyretin cardiac amyloidosis among the different Perugini grades? *Hell J Nucl Med* 2023; 26(3): 172-80.
10. Violet J, Jackson P, Ferdinandus J et al. Dosimetry of ^{177}Lu-PSMA-617 in Metastatic Castration-Resistant Prostate Cancer: Correlations Between Pretherapeutic Imaging and Whole-Body Tumor Dosimetry with Treatment Outcomes. *J Nucl Med* 2019; 60(4): 517-23.
11. Yamane T, Fukushima K, Shirotake S et al. Test-retest repeatability of quantitative bone SPECT/CT. *Ann Nucl Med* 2021; 35(3): 338-46.
12. Ritt Recent Developments in SPECT/CT. *Semin Nucl Med* 2022; 52(3): 276-85.
13. Koppula BR, Morton KA, Al-Dulaimi R et al. SPECT/CT in the Evaluation of Suspected Skeletal Pathology. *Tomography* 2021; 7(4): 581-605.
14. Tzortzakakis A, Holstensson M, Hagel E et al. Intra- and Interobserver Agreement of SUV SPECT Quantitative SPECT/CT Processing Software, Applied in Clinical Settings for Patients with Solid Renal Tumors. *J Nucl Med Technol* 2019; 47(3): 258-62.
15. Kitajima K, Futani H, Komoto H et al. Quantitative bone SPECT/CT applications for primary bone neoplasms. *Hell J Nucl Med* 2021; 24(1): 36-44.
16. Ikeda T, Kitajima K, Tsuchitani T et al. Effectiveness of quantitative bone SPECT/CT for bone metastasis diagnosis. *Hell J Nucl Med* 2022; 25(3): 253-9.
17. Ryoo HG, Lee WW, Kim JY et al. Minimum Standardized Uptake Value from Quantitative Bone Single-Photon Emission Computed Tomography/Computed Tomography for Evaluation of Femoral Head Viability in Patients with Femoral Neck Fracture. *Nucl Med Mol Imaging* 2019; 53(4): 287-95.
18. Tabotta F, Jreige M, Schaefer N et al. Quantitative bone SPECT/CT: high specificity for identification of prostate cancer bone metastases. *BMC Musculoskelet Disord* 2019; 20(1): 619.
19. Qi N, Pan B, Meng Q et al. Deep learning enhanced ultra-fast SPECT/CT bone scan in patients with suspected malignancy: quantitative assessment and clinical performance. *Phys Med Biol* 2023; 68(13).
20. Zhang Q, Xu W. Correlation analysis of I-131 SPECT/CT uptake parameters with the success ablation treatment of thyroid remnant in patients with low-intermediate-risk differentiated thyroid cancer. *Nucl Med Commun* 2022; 43(10): 1051-7.
21. Brady SL, Shulkin BL. Analysis of quantitative [I-123] mIBG SPECT/CT in a phantom and in patients with neuroblastoma. *EJNMMI Phys* 2019; 6(1): 31.
22. Zeng T, Gao J, Gao D et al. A GPU-accelerated fully 3D OSEM image reconstruction for a high-resolution small animal PET scanner using dual-ended readout detectors. *Phys Med Biol* 2020; 65(24): 245007.
23. Tsuda K, Suzuki T, Toya K et al. 3D-OSEM versus FORE+OSEM: Optimal Reconstruction Algorithm for FDG PET with a Short Acquisition Time. *World J Nucl Med* 2023; 22(3): 234-43.
24. Law SK. Traditional, Complementary, and Integrative Medicines in the USA for COVID-19. *J Mod Nurs Pract Res* 2023; 3(2): 10.